Research Square

Preprints are preliminary reports that have not undergone peer review.
They should not be considered conclusive, used to inform clinical practice,
or referenced by the media as validated information.

Energy-Efficient Degradation of Tetracycline Using Plasma-Activated Water Generated by a Multi-Jet DBD Diffuser

Zeinab Ansari
Shiraz University
Mohammad Mohammad Hosseini
Shiraz University
Fatemeh Ranjbar Nezam Abadi
Shiraz University
Hamed Taghvaei
taghvaei.h@shirazu.ac.ir

Shiraz University

Article

Keywords: Plasma-activated water (PAW), Non-thermal plasma (NTP), Dielectric barrier discharge (DBD), Tetracycline hydrochloride (TCH), water treatment, advanced oxidation process (AOP)

Posted Date: November 20th, 2026

DOI: https://doi.org/10.21203/rs.3.rs-11639741/v1

License: This work is licensed under a Creative Commons Attribution 4.0 International License.
Read Full License

Additional Declarations: No competing interests reported.

Energy-Efficient Degradation of Tetracycline Using Plasma-Activated Water Generated by a Multi-Jet DBD Diffuser

Zeinab Ansari, Mohammad Mohammad Hosseini, Fatemeh Ranjbar Nezam Abadi, Hamed Taghvaei*

Department of Chemical Engineering, Shiraz University, Shiraz 71345, Iran

*Corresponding Authors:
E-mail: taghvaei.h@shirazu.ac.ir (Hamed Taghvaei)

Abstract:

tetracycline hydrochloride (TCH) is a widely used antibiotic that persists in aquatic environments due to its chemical stability and low removal efficiency in conventional treatment systems, raising environmental and health concerns and highlighting the need for fast, energy-efficient treatment methods. Non-thermal plasma is a promising advanced oxidation technology that generates reactive oxygen and nitrogen species under mild conditions. Plasma-activated water (PAW), produced by transferring these species into the liquid phase, provides strong oxidative potential for degrading recalcitrant pollutants. In this study, a multi-array dielectric barrier discharge (DBD) plasma jet diffuser was employed to generate PAW for TCH degradation. The reactor enabled direct plasma-assisted bubbling inside the solution, improving gas–liquid mass transfer and reactive species formation. The effects of input power, air flow rate, processing time, solution volume, and PAW storage were systematically evaluated. Considering TCH removal efficiency and energy efficiency, the optimal condition was 3 W input power, 700 mL/min air flow rate, 30 s processing time, and 100 mL solution volume, achieving 71.48% TCH removal and approximately 20 g/kWh energy efficiency. Reactive species analysis confirmed that dissolved ozone played a dominant role, while rapid oxidant decay during storage highlighted the need for immediate PAW utilization.

Keywords: Plasma-activated water (PAW); Non-thermal plasma (NTP); Dielectric barrier discharge (DBD); Tetracycline hydrochloride (TCH); water treatment, advanced oxidation process (AOP).

1. Introduction

Water contamination by pharmaceutical residues has emerged as a growing global concern, driven by the widespread consumption of antibiotics and their continuous discharge into municipal and industrial wastewater streams (Griffero et al. 2026; Mandlazi et al. 2026). These bioactive compounds are designed to be chemically stable and biologically active at low concentrations, properties that make them persistent in aquatic environments and capable of exerting adverse ecological and toxicological impacts (Ali et al. 2026). Among pharmaceutical pollutants, tetracycline hydrochloride (TCH), one of the most extensively used broad-spectrum antibiotics, is frequently detected in wastewater effluents, surface waters, and even groundwater (Kayani 2025; Semenova et al. 2025). Its high solubility, resistance to biodegradation, and tendency to promote the propagation of antibiotic-resistant bacteria highlight the urgent need for effective treatment strategies capable of degrading or transforming such contaminants (Li et al. 2024; Wang et al. 2024).

Conventional wastewater treatment technologies can generally be categorized into physical, biological, and chemical processes (Amparán et al. 2025). Physical treatment methods such as sedimentation, filtration, adsorption, and membrane separation primarily rely on the separation of contaminants from the water phase rather than their chemical destruction (Łukasiewicz 2025). Although these techniques can effectively reduce turbidity and remove certain pollutants, they often face limitations when dealing with dissolved and structurally stable organic compounds and may generate secondary waste streams that require additional treatment (Crini et al. 2026). Biological treatment processes are widely applied due to their relatively low operational costs and environmental compatibility; however, their efficiency is often restricted when treating wastewater containing persistent pharmaceutical compounds (Dolatimehr et al. 2024; Islam et al. 2025).

Antibiotics such as tetracycline may inhibit microbial activity and exhibit limited biodegradability, which reduces the effectiveness of biological degradation pathways (Hidayatullah et al. 2025).

Chemical treatment methods offer the advantage of transforming pollutants through oxidation, reduction, or other chemical reactions, enabling the breakdown of complex organic molecules into less harmful compounds (Ethiraj et al. 2024; Rasool et al. 2025). Among chemical treatment strategies, advanced oxidation processes (AOPs) have attracted significant attention due to their ability to generate highly reactive oxidizing species capable of attacking stable organic structures (Satyam and Patra 2025; Wang et al. 2025). These processes are characterized by the production of powerful oxidants, particularly hydroxyl radicals and other reactive oxygen species, which can rapidly degrade a wide range of refractory organic contaminants (Silva 2025). As a result, AOPs have emerged as an effective and promising approach for the treatment of wastewater containing persistent pharmaceutical residues.

Within this group, non-thermal plasma (NTP) technologies have emerged as an environmentally friendly and energy-efficient option. NTP can produce a diverse range of reactive oxygen and nitrogen species (RONS), including ozone, hydroxyl radicals, hydrogen peroxide, nitric oxides, and other long-lived oxidants, under ambient temperature and pressure without chemical additives (Hossaini et al. 2024; Xu and Bassi 2025). These species can initiate complex oxidation pathways that lead to the breakdown of antibiotic structures and the formation of less harmful intermediates.

Plasma-activated water (PAW), obtained by exposing water to non-thermal plasma prior to its use in treatment, offers a versatile indirect approach for harnessing plasma-generated reactive species. PAW contains a mixture of long-lived oxidants such as nitrate, nitrite, hydrogen peroxide, peroxynitrite, and dissolved ozone, which collectively contribute to its oxidative potential (Kumar and Saxena 2026). The ability to generate PAW independently of the contaminated matrix provides

operational flexibility, improved safety, and enhanced control over treatment conditions compared with direct plasma–liquid interactions (Zou et al. 2025).

In recent years, bubble-assisted plasma diffuser designs have been explored to enhance the mass transfer of reactive species from the gas phase to the liquid (Chen et al. 2026). Multi-jet dielectric barrier discharge (DBD) plasma diffusers integrated into bubble column reactors can disperse gas into fine bubbles, significantly increasing the interfacial area and promoting the dissolution and stabilization of RONS in the liquid phase (Mbanugo et al. 2025). Such configurations improve the oxidative strength of PAW while enabling more uniform distribution of reactive species throughout the treated volume.

A growing body of research has demonstrated the strong potential of plasma-based systems for the degradation of tetracycline. Amina Ouzar et al. employed a gliding arc non-thermal plasma combined with iron-based catalysts, achieving complete degradation at 50 ppm within 15 min using plasma–Fe(VI), while plasma–Fe(II) reached 97.28 % removal after 30 min (Ouzar et al. 2025). In related work, Ouzar and Kim used a gliding arc discharge system and obtained 94.95 % tetracycline degradation and 81.3 % mineralization at an initial concentration of 5 mg/L within 30 min (Ouzar and Kim 2022). Jing Lou et al. applied a dielectric barrier discharge plasma coupled with biochar derived from *Enteromorpha prolifera*, where the DBD/BC600 configuration achieved 89.36 % removal with an energy yield of 6.21 g/kWh in only 5 min (Lou et al. 2021). Dong He et al. integrated corona discharge plasma with TiO_2 synthesized via sol–gel and reported an increase in tetracycline removal from 61.9 % to 85.1 % at 36 W within 24 min for a 50 mg/L solution, alongside an improvement in TOC removal from 25.3 % to 53.4 % (He et al. 2014). Huang et al. showed that adding 0.25 mmol/L hydroxylamine to a discharge plasma system enhanced overall degradation from 70.7 % to 90.0 % and increased energy efficiency from 2.28 to 3.18 g/kWh (Huang

et al. 2022). Similarly, Chunjing Hao et al. used a pulsed coaxial dielectric barrier discharge reactor with a screw-type electrode and achieved 92.3 % degradation and 65.01 % TOC removal at 50 mg/Lwith an energy efficiency of 20.24 g/kWh (Hao et al. 2020).

Although numerous studies have demonstrated the effectiveness of plasma-based technologies for tetracycline degradation, most investigations have focused on direct plasma treatment, where the antibiotic solution is directly exposed to plasma discharge within different reactor configurations. While these approaches have shown considerable degradation efficiency, the indirect treatment strategy based on plasma-activated water (PAW) has received comparatively limited attention. Consequently, the potential of PAW as an alternative oxidizing medium for tetracycline removal, as well as the influence of key operational parameters on its treatment performance and energy efficiency, remains insufficiently explored.

In our previous works, we designed and fabricated the multi-jet dielectric barrier discharge plasma diffuser integrated into a bubble column reactor, focusing on the investigation of post-discharge effects for pollutant degradation (Kazemi and Taghvaei 2021; Hosseini and Taghvaei 2025; Rezaee et al. 2026). Building upon these design principles, the present study represents the first application of our previously fabricated multi-jet DBD plasma diffuser for PAW generation followed by its use for tetracycline hydrochloride (TCH) degradation. The effects of key operating parameters, including input power, air flow rate, and activation time, were systematically investigated with emphasis on removal efficiency and energy performance. Additionally, variations in ozone concentration, nitrogenous species formation, pH changes, and PAW storage stability were analyzed to provide a clearer understanding of the factors governing tetracycline degradation in PAW-based treatment systems.

2. Materials and methods

2.1 Chemical and materials

Tetracycline hydrochloride (TCH) used in this study was obtained in high-purity crystalline powder form from Merck (Germany). The compound appears as a yellow crystalline solid and was used without any further purification. All other chemicals and reagents employed throughout the experiments, including standards and analytical-grade materials, were supplied by Merck or Sigma-Aldrich and met the required purity specifications for analytical applications. To minimize interference from background ions and ensure high reproducibility and accuracy across all measurements, double-distilled water was used to prepare solutions and throughout the experimental procedures. The physicochemical properties of tetracycline hydrochloride relevant to this study are summarized in Table 1.

Table 1. Physical and chemical properties of tetracycline

Property	**Value**
Molecular formula	C22H24N2O8·HCl
Molecular weight ($\frac{g}{mol}$)	480.90
Appearance	Yellow crystalline powder
Solubility in water	Highly soluble
Melting point (°C)	220–235

2.2 Experimental setup

A schematic representation of the experimental configuration is shown in Fig. 1. The system included a bubble column reactor integrated with a multi-jet dielectric barrier discharge (DBD) plasma diffuser designed for PAW production. In this arrangement, the diffuser served as a

non-thermal plasma generator that produced reactive gas-phase species with low power consumption, which were then transferred into the liquid medium via rising gas bubbles.

The plasma diffuser consisted of a central stainless-steel rod electrode positioned coaxially within some quartz capillary tubes (outer diameter 2 mm, inner diameter 1 mm, length 10 cm). Silicone insulating material was applied to the annular region between the rod electrode and the surrounding tubes to prevent electrical sparking or direct discharge. A layer of copper foil wrapped around the outer surfaces of the quartz tubes functioned as the high-voltage electrode, while the inner rod was connected to ground. For additional electrical insulation and operator safety, the outer electrode was encased within a protective rubber sheath.

Air was selected as the feed gas and delivered from beneath the quartz tubes using a flexible rubber connector, ensuring uniform dispersion into each capillary. The diffuser was positioned at the base of a cylindrical Plexiglas bubble column (internal diameter 4.4 cm, height 15 cm), providing maximum interaction between gas bubbles and the liquid phase. A minimum airflow of 300 mL/min was required to achieve simultaneous bubble formation from all capillaries. The internal air pressure and small tube diameter prevented backflow of liquid into the discharge region even during brief interruptions of gas supply, maintaining a dry environment essential for stable plasma formation.

Both ends of the reactor were sealed with Teflon fittings. The top fitting allowed sampling and periodic measurement of ozone, nitrite, and nitrate concentrations generated throughout plasma exposure.

A high voltage power supplier (AC, with the frequency of 20 kHz) is used to generate a sinusoidal signal. Real-time monitoring of applied voltage and transferred charge was performed using a dual-

channel Tektronix TDS1012B-SC oscilloscope (100 MHz bandwidth, 1.0 GS/s sampling rate). Voltage was measured with a Tektronix P6015A high-voltage probe. To enable precise calculation of charge transfer, a 1 pF capacitor was installed in series with the inner electrode. Instantaneous voltage, current, and energy consumption were recorded throughout plasma operation to evaluate the electrical behavior of the system and ensure reproducibility of reactive species generation.

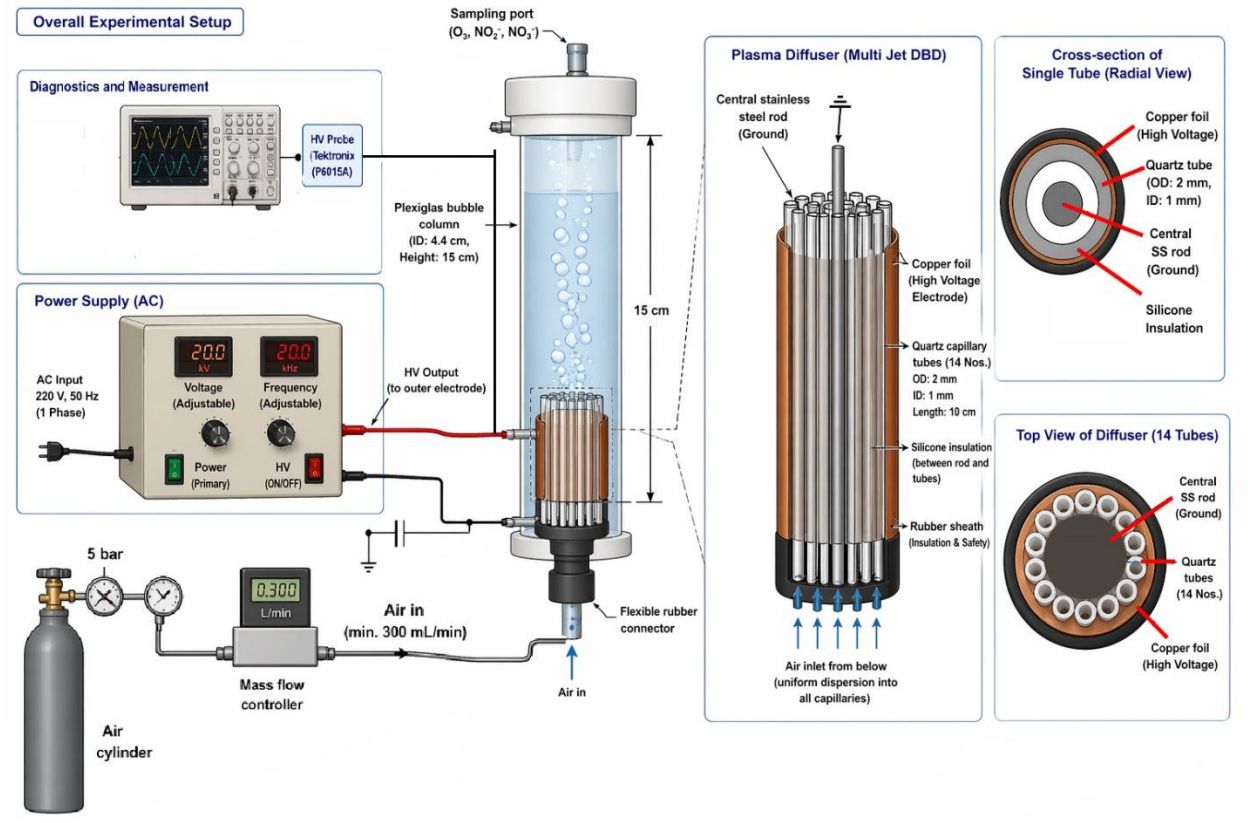


Fig. 1. *The schematic of the experimental setup.*

2.3 Analysis method

The concentration of TCH in the treated samples was determined using a UV–Visible spectrophotometer (UV/Vis 2150, Unico). Measurements were performed at the maximum

absorption wavelength of TCH, corresponding to 356 nm. A calibration curve was established using a series of standard TCH solutions with known concentrations, and this curve was employed to quantify TCH concentration in each collected sample.

The removal efficiency of tetracycline hydrochloride was calculated using Eq. 1 (Solouki et al. 2026):

$$\text{Removal (\%)} = \frac{C_0 - C_t}{C_0} \times 100 \qquad (1)$$

where R, C_0, and $C_t$represent the removal efficiency of TCH (%), initial TCH concentration (ppm), and post-treatment TCH concentration (ppm), respectively.

The energy efficiency of the plasma treatment system, expressed as the mass of pollutant removed per unit of electrical energy supplied, was evaluated using Eq. (2) (Kumar et al. 2024; Ben Amor et al. 2025):

$$\text{Energy efficiency } \left(\frac{g}{kW.h}\right) = \frac{C_0 \times V \times \frac{1}{100} \times R}{P \times t} \qquad (2)$$

Where C_0, V, R, P, and t represent initial solution concentration (g/L), solution volume (L), removal efficiency of TCH (%), input power (kW), and treatment time (h), respectively.

2.3.1 Input power

The average power delivered to the plasma reactor was determined from the voltage and current waveforms captured by the oscilloscope. The calculation was carried out by numerically integrating the product of instantaneous voltage and current over each pulse period, as expressed in Eq. (3) (Minesi et al. 2022; Alegria 2023):

$$P_{\text{ave}}(kW) = f \times \sum_{i=0}^{n} \frac{(V_i + V_{i+1})}{2} \times \frac{(I_i + I_{i+1})}{2} \times (t_{i+1} - t_i) \qquad (3)$$

In this expression, f denotes the pulse repetition frequency (kHz). The terms V_i and V_{i+1} correspond to two successive voltage samples obtained from the oscilloscope (kV), while I_i and I_{i+1} represent the discharge current values recorded at the same sampling points (A). The difference $t_{i+1} - t_i$ indicates the time interval between these adjacent waveform points (s), which forms the basis for the numerical integration used to estimate the average input power. Throughout all experiments, the pulse repetition frequency was fixed at 20 kHz to ensure stable plasma operation.

2.3.2 Measurement of ozone concentration

The concentration of dissolved ozone in the plasma-treated water was quantified using the indigo colorimetric technique. To prepare the samples, 100 mL of distilled water was first subjected to plasma exposure to produce ozonated plasma-activated water. Then, 20 mL of the indigo reagent was added to 80 mL of this ozone-containing water, allowing the dye to react with dissolved ozone. The absorbance of the resulting mixture was subsequently recorded at 600 nm using a UV–Visible spectrophotometer. The reduction in absorbance, compared with a control solution prepared by mixing the same amount of indigo with non-ozonated distilled water, provided the basis for calculating the ozone concentration in the liquid phase.

The concentration of dissolved ozone was obtained using Eq. (4) (Bader 1982):

$$\text{Ozone concentration (mg/L)} = \frac{100 \times \Delta A}{f \times b \times V} \qquad (4)$$

In this equation, ΔA represents the difference in absorbance between the ozone-reacted indigo solution and the control sample; f denotes the sensitivity coefficient of the indigo method (0.42

L/mg.cm); $b$is the optical path length of the cuvette (cm); and V corresponds to the sample volume used for analysis (mL), which in this study was 80 mL.

2.3.3 Measurement of nitrogenous species

The nitrogenous species produced in the exhaust gas stream of the plasma diffuser were quantified using a Testo 350 gas analyzer. During each measurement, the gas exiting the reactor was continuously directed into the sampling probe of the instrument, allowing the analyzer to detect and report the concentrations of the relevant nitrogen-containing compounds in real time. The device provided direct digital readouts, enabling rapid assessment of both the generated species and their consumption during plasma operation.

2.4 Experimental Procedure

Before initiating the discharge, the gas stream was allowed to fully fill the plasma diffuser to avoid ignition instability. The power supply was subsequently activated and adjusted to the desired voltage level, after which the system was allowed to reach a steady and stable plasma state. Throughout each experiment, the input power was continuously monitored, and the applied voltage was fine-tuned when necessary to maintain the prescribed power setting.

For plasma activation, 100 mL of distilled water was transferred into the bubble-column reactor and exposed to plasma under the selected operating conditions. After completing the predetermined treatment period, the generated plasma-activated water (PAW) was immediately collected from the reactor outlet.

In a separate step, 40 mL of TCH solution with an initial concentration of 17.5 ppm was prepared. The freshly obtained 100 mL of PAW was immediately mixed with the TCH solution, yielding a total reaction volume of 140 mL and an initial TCH concentration of 5 ppm in the reaction mixture.

The mixture was gently stirred to ensure homogeneous distribution of the reactive species throughout the solution.

The remaining concentration of TCH after reaction was quantified using UV–Visible spectrophotometry at its characteristic absorption wavelength of 356 nm, based on a previously established calibration curve. All analytical measurements were carried out under identical conditions to ensure consistency.

The main degradation experiments were conducted in triplicate under identical experimental conditions. Data are presented as mean ± standard deviation (SD), and the error bars represent the standard deviation of the replicate measurements.

3. Results and Discussion

3.1 Effect of Input Power and Processing Time

To evaluate the influence of input power and plasma exposure time on the degradation performance of the atmospheric DBD plasma diffuser, a series of experiments was conducted under a constant air flow rate of 500 mL/min. The input power was varied between 3 and 5 W, while the treatment times were set to 30 s, 1, 5, and 10 min.

Fig. 2A illustrates the effect of input power on TCH removal efficiency, and the corresponding energy efficiency is shown in Fig. 2B. As illustrated in Fig. 2A, TCH degradation efficiency strongly depended on the applied input power. At 3 W (plasma breakdown power), the removal efficiency reached its highest value, whereas a further increase in power to 5 W caused a pronounced decline in performance, with removal efficiencies falling below 10% under all treatment times. A similar trend was observed for energy efficiency (Fig. 2B), where the maximum

value was obtained at the lowest power level and then decreased sharply with increasing input power.

This inverse relationship between power and degradation efficiency primarily arises from the thermal effects associated with elevated discharge energy. As input power increases, part of the supplied electrical energy is dissipated as heat rather than being utilized for the gas ionization and formation of reactive species. As the power increases from 3 to 5 W, the maximum reactor temperature rises from 49.8 °C to 65.2°C after 1 min treatment time. The elevated reactor temperature significantly accelerates the thermal decomposition of key oxidizing species, particularly ozone, in the plasma discharge and shortens its lifetime in the liquid phase, thereby leading to weakened oxidative degradation of TCH (see sections 3.4.2 and 3.5) (Naudé et al. 2005; Levanov et al. 2019; Elaissi and Alsaif 2023). The reduction in the liquid's dielectric constant at elevated temperatures can also alter the discharge characteristics at the plasma–liquid interface, thereby further suppressing the generation of reactive species (Hosseini and Taghvaei 2025).

Moreover, excessive energy input intensifies secondary gas-phase reactions that promote the recombination of reactive oxygen and nitrogen species (RONS). This process limits the net production of long-lived oxidants such as O_3, NO_2^-, and NO_3^-, reducing their steady-state concentrations in the plasma effluent (Lunder et al. 2025). As a result, the PAW's oxidation capacity decreases.

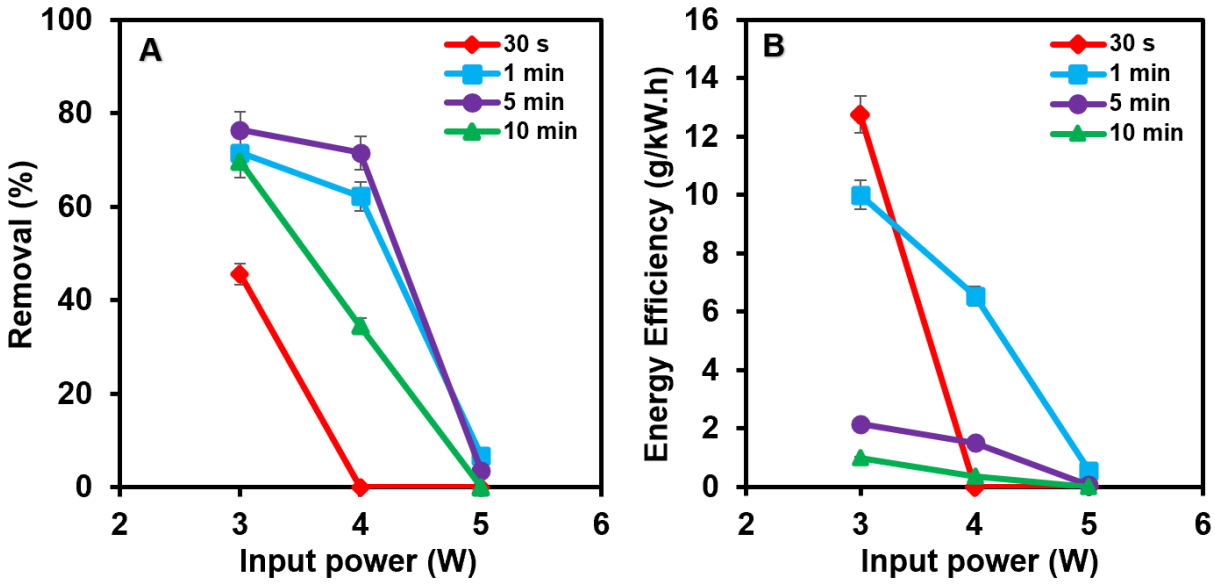


Fig. 2. *Effect of input power on (A) TCH removal efficiency and (B) energy efficiency at an air flow rate of 500 mL/min and treatment times of 30 s, 1 min, 5 min, and 10 min.*

Furthermore, the treatment time had a noticeable effect on TCH degradation only at the initial stage of plasma activation, where increasing the processing time from 30 s to 1 min improved the removal performance. However, extending the treatment beyond 1 min did not produce a proportional enhancement. This behavior can be attributed to several factors. First, prolonged plasma operation likely caused gradual heating of the reactor and outlet gas, which may have accelerated the decomposition of key oxidizing species, particularly ozone, in the plasma discharge, while also reducing their solubility and lifetime in the liquid phase (see section 3.4.1). Thermographic imaging and the corresponding temperature profiles confirm this hypothesis (Fig. 3). As the treatment time increases from 0.5 to 10 min, the maximum reactor temperature rises from 45.3°C to 85°C, while the outlet gas temperature at the reactor nozzle rises from 32°C to 40°C. Second, the concentration of reactive species generated in the PAW may have approached

saturation, so that additional exposure time did not significantly increase the amount of available oxidants. In addition, as the concentration of active species in the liquid increased, the mass-transfer driving force for diffusion from the gas phase to the liquid phase became weaker, making further dissolution of reactive species progressively less efficient. Third, the continuous decline in pH with longer treatment times may have altered the chemical environment of the solution and changed the stability and reactivity of plasma-generated species.

The variation in pH during plasma activation plays a crucial role in determining the degradation behavior of tetracycline hydrochloride (TCH). As the treatment proceeds, the dissolution of reactive nitrogen species such as NOx into the liquid phase leads to the formation of acidic species, mainly nitrous and nitric acids, which markedly decrease the solution pH. This acidification not only alters the speciation of TCH but also affects the stability and reactivity of plasma-generated oxidants. Since TCH is an amphoteric compound with pKa values of 3.3, 7.7, and 9.7, a low-pH environment favors its protonated forms, which may influence its interaction with oxidizing species in PAW. In addition, acidic conditions can enhance the persistence of dissolved ozone to some extent, while excessive acidification may simultaneously suppress the indirect generation of hydroxyl radicals from ozone.

As shown in Fig. 4, the pH of PAW decreased continuously as a function of activation duration when operated at 3 W input power, an airflow rate of 500 mL/min. The pH declined from approximately 4.4 at 30 s to 3.4 after 10 min, reflecting the well-established acidification behavior characteristic of air-fed nonthermal plasma systems. This acidification originates from the dissolution of plasma-generated reactive nitrogen species (RNS) such as NO, NO_2, and NO_3, followed by their oxidation through long-lived oxidants including ozone and hydrogen peroxide, ultimately yielding nitrous (HNO_2) and nitric (HNO_3) acids. The accumulation of these

nitrogen-containing acidic species accounts for the steady decline in pH (Thirumdas et al. 2018; Al-Sharify et al. 2020).

The time-dependent nature of this process is also evident. During the initial stage of plasma exposure, acid formation occurs rapidly because the production of RNS and their dissolution into the aqueous phase proceed at a relatively high rate, causing a pronounced early drop in pH. As activation time extends beyond several minutes, the rate of pH reduction becomes slightly attenuated, suggesting that continuous acid production is partially balanced by the concurrent consumption or recombination of reactive species in solution. Therefore, the observed time dependence suggests that a short activation period is sufficient to generate an effective oxidative medium, while longer treatment times mainly increase energy consumption without yielding a meaningful improvement in TCH degradation. This confirms that the process is governed by an early-stage generation of reactive species followed by limited marginal gains due to thermal effects, species saturation, and pH-driven chemical changes.

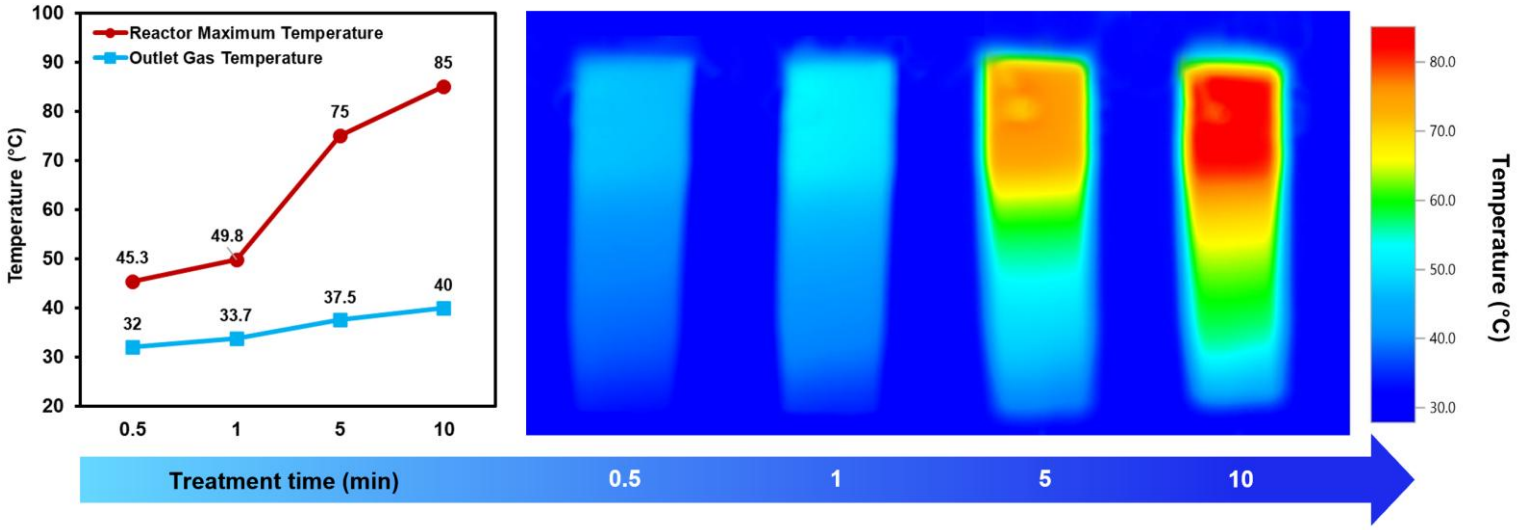


Fig. 3. *Thermographic imaging and the corresponding temperature profiles of reactor and outlet gas temperature.*

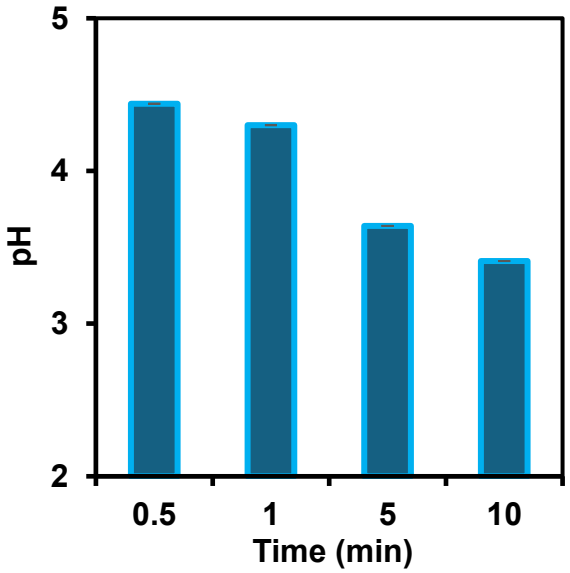


Fig. 4. *Temporal evolution of pH in plasma-activated water generated at an input power of 3 W and an airflow rate of 500 mL/min for different plasma activation durations (30 s–10 min).*

3.2 Effect of flow rate

Following the identification of 30 s and 1 min as the most energy-efficient treatment durations, the influence of gas flow rate on the performance of the atmospheric DBD plasma diffuser was examined at a constant input power of 3 W. As illustrated in Fig. 5A, the removal efficiency of TCH exhibited a clear dependence on the airflow rate. Increasing the flow rate from 500 to 900 mL/min led to a measurable improvement in degradation for both treatment durations. For a treatment time of 30 s, the removal efficiency rose from 46% at 500 mL/min to 74% at 900 mL/min. A comparable trend was observed for 1 min, where the removal efficiency increased from 72% to 76% within the same flow range.

This enhancement can be attributed to the increased density of feed gas molecules entering the discharge region, which promotes more frequent electron–molecule collisions and thereby elevates the production rate of reactive oxygen and nitrogen species (RONS). Additionally, higher flow rates intensify microbubble formation and liquid mixing, improving gas–liquid interfacial transport and facilitating the dissolution of long-lived oxidants such as ozone and hydrogen peroxide (Chen et al. 2009, 2017; Jiang et al. 2012). These combined effects ultimately strengthen the oxidative potential of the PAW and accelerate TCH degradation.

However, when the airflow was further increased to 1200 mL/min, a decline in removal efficiency was observed. At 30 s, the efficiency decreased to 66.5%, while at 1 min, it dropped to 62%. The reduction at elevated airflow rates is primarily associated with the shorter residence time of gas bubbles in the active discharge zone, which restricts both the plasma–gas interaction time and the formation of key reactive species (Basu-Modak et al. 2006; Aboubakr et al. 2016). Moreover, rapid gas passage promotes the formation of larger bubbles, diminishing interfacial contact area and limiting mass transfer of oxidants into the liquid environment, ultimately reducing the oxidation capacity of the PAW (Kazemi and Taghvaei 2021) (see sections 3.4.3 and 3.5).

The corresponding energy efficiencies are presented in Fig. 5B. For 30 s, the energy efficiency increased from 12.76 g/kW.h at 500 mL/min to approximately 20.01 g/kW.h at both 700 and 900 mL/min, followed by a decrease to 18.46 g/kW.h at 1200 mL/min. For 1 min, the efficiency remained nearly constant at 10.01 g/kW.h for 500 and 700 mL/min, slightly increased to 10.53 g/kW.h at 900 mL/min, and then declined to 8.97 g/kW.h at 1200 mL/min.

Considering both removal performance and energy efficiency, the optimal operational point is achieved at a flow rate of 700 mL/min under 3 W input power, where the system provides the highest removal efficiency together with favorable energy performance. This outcome underscores the importance of balancing gas residence time and reactive species generation to maximize the oxidative capability of PAW.

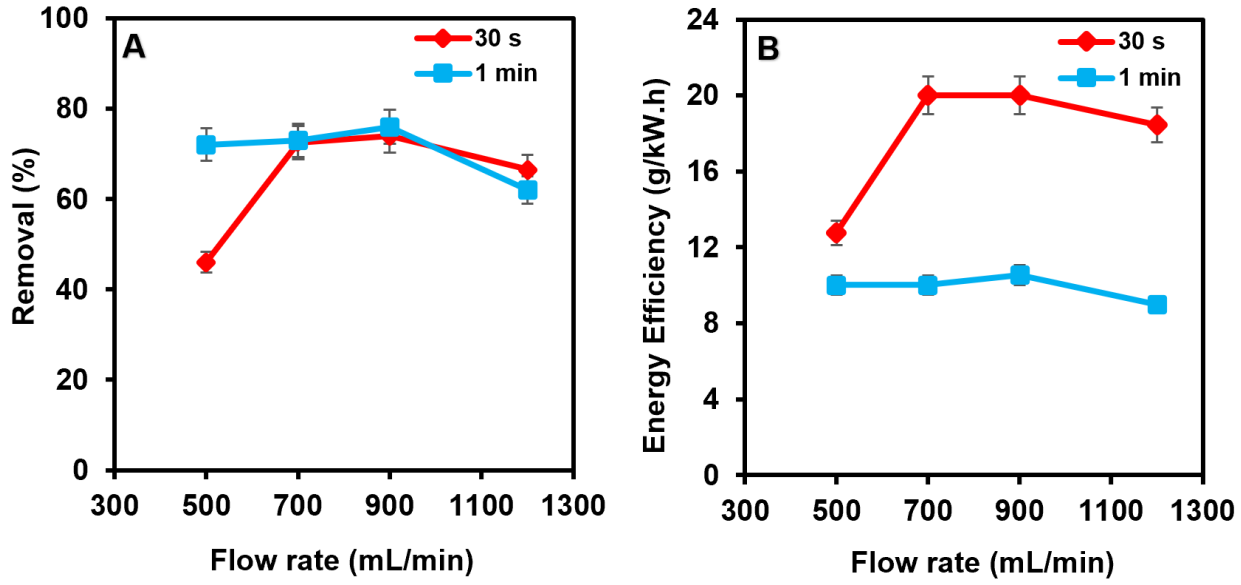


Fig. 5. *Effect of air flow rate on (A) TCH removal efficiency and (B) energy efficiency at an input power of 3 W and treatment durations of 30 s and 1 min.*

3.3. Stability of plasma-activated water

The storage stability of PAW under optimal plasma-generation conditions 3 W input power, 500 mL/min airflow, and 1 min activation time is illustrated in Fig. 6. A rapid decline in TCH removal efficiency was observed as storage time increased. Immediately after generation, the degradation efficiency reached 71.48%, but this performance diminished to 12% after 15 min, 4% after 30 min, and 1.5% after 45 min, eventually approaching negligible activity after one hour of storage.

This pronounced loss of reactivity is directly linked to the limited lifetime and progressive depletion of the oxidizing species responsible for TCH degradation. Among them, ozone, identified as a dominant long-lived species in PAW, typically persists only for several minutes to tens of minutes in aqueous environments (see section 3.4.4). Other contributors, including H_2O_2, NO_2^-, and peroxynitrite, also undergo spontaneous breakdown or participate in secondary reactions that steadily reduce their oxidizing power (Zhou et al. 2020). As a result, the concentration of these key reactive species diminishes with storage time, leading to a substantial decline in the overall oxidative capability of PAW.

Taken together, these findings demonstrate that freshly generated PAW exhibits the highest reactivity toward TCH, whereas extended storage even within the first 15–30 min significantly compromises its treatment performance.

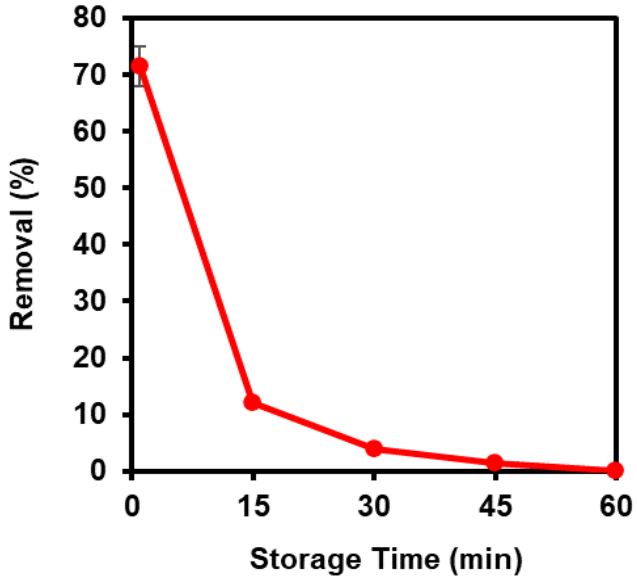


Fig. 6. *Variation of TCH removal efficiency as a function of PAW storage time under optimal operating conditions (3 W input power, 500 mL/min airflow, 1 min activation).*

3.4. Effect of Dissolved Ozone Concentration

For the role of ozone in the degradation of TCH to be ascertained, the temporal behavior of dissolved O_3 and its dependence on plasma operating conditions were thoroughly examined. Ozone is a primary long-lived oxidant that is produced in air-based atmospheric plasma systems. It functions as a precursor for various secondary reactive species in the aqueous phase. In dielectric-barrier configurations powered by AC high voltage, the production of O_3 is primarily attributed to electron-induced dissociation of O_2, followed by three-body recombination. After its production, a portion of the gaseous O_3 diffuses through the bubble-liquid interface and dissolves in the aqueous phase. In this phase, O_3 may either remain intact or decompose, thereby generating more reactive radicals (Wu et al. 2018; Yang et al. 2018). The interplay between these generations and decay pathways determines the final measurable concentration in PAW.

3.4.1. Influence of Plasma Activation Time on Dissolved Ozone

Fig. 7A displays the variation of dissolved ozone at 500 mL/min airflow and an input power of 3 W for different activation durations. At the beginning of treatment, the dissolved O_3 level increases rapidly, rising from approximately 0.48 mg/L at 30 s to a peak of 0.78 mg/L at 5 min. This upward trend reflects the progressive accumulation of O_3 generated in the gas phase and efficiently transferred into the liquid due to strong gas–liquid contact in the bubble column reactor. However, after 5 min, the concentration begins to drop, decreasing to about 0.70 mg/L at 10 min. This decline indicates that decomposition reactions gradually dominate at longer treatment times. Once dissolved, O_3 participates in a range of aqueous-phase processes, including reactions with nitrogenous intermediates and self-decomposition. The consumption of O_3 at longer durations parallels the slight decline in TCH removal beyond the optimum activation time, confirming the strong association between the availability of dissolved oxidants and degradation efficiency. Additionally, the decrease in pH resulting from the dissolution of nitrogen oxides at longer treatment time (discussed in previous sections) can contribute to ozone absorption reduction in the aqueous phase.

3.4.2. Influence of Input Power on Dissolved Ozone

The influence of input power on dissolved ozone is illustrated in Fig. 7B for a fixed activation time of 1 min at 500 mL/min. When input power is increased from 3 W to 4 W, O_3 decreases from 0.50 mg/L to 0.36 mg/L, and further drops to 0.18 mg/L at 5 W. Elevating the applied power raises the local gas temperature inside the plasma channel, which accelerates thermal decomposition of O_3 and simultaneously suppresses its solubility in water (Mok et al. 2008; Rahimpour et al. 2019). This is consistent with the sharp reduction in TCH removal observed under the same conditions.

3.4.3. Influence of Airflow Rate on Dissolved Ozone

Fig. 7C presents the effect of airflow rate on dissolved ozone concentration together with the corresponding TCH removal efficiency obtained after 30 s of plasma activation. For both activation durations (30 s and 1 min), the dissolved O_3 concentration initially increased as the airflow rate was raised from 500 to 700 mL/min, reaching maximum values of approximately 0.41 and 0.60 mg/L, respectively. Further increasing the airflow rate resulted in a gradual decline in dissolved ozone, with concentrations decreasing to approximately 0.34 mg/L (30 s) and 0.43 mg/L (1 min) at 1200 mL/min.

The initial increase in dissolved ozone is attributed to the enhanced supply of oxygen molecules to the discharge region, together with improved gas dispersion, which promotes ozone formation and its transfer into the liquid phase. However, at excessive airflow rates, the residence time of the gas inside the plasma discharge becomes shorter, reducing the probability of electron-impact reactions responsible for ozone generation. Moreover, the formation of larger and faster-rising bubbles decreases the gas–liquid contact time and limits ozone dissolution into the aqueous phase (Jo et al. 2015). Interestingly, the variation in TCH removal efficiency does not completely follow the dissolved ozone profile. Although the highest dissolved ozone concentration was observed at an airflow rate of 700 mL/min, the removal efficiency remained nearly unchanged at 900 mL/min before declining at 1200 mL/min. This behavior indicates that ozone is the dominant but not the sole oxidizing species involved in TCH degradation. At 900 mL/min, the enhanced hydrodynamic conditions likely improve the transport of other plasma-generated reactive species, including H_2O_2, NO_2^-, $ONOO^-$, and secondary radicals produced through ROS–RNS interactions, partially compensating for the slight decrease in dissolved ozone. These findings suggest that the

degradation performance of PAW is governed by the combined effects of ozone concentration, reactive nitrogen species, and gas–liquid mass transfer rather than by dissolved ozone alone.

3.4.4. Storage stability of dissolved ozone

The storage stability of dissolved ozone and its relationship with TCH removal efficiency are presented in Fig. 7D. Immediately after plasma activation, the dissolved O_3 concentration reached approximately 0.50 mg/L, accompanied by a TCH removal efficiency of 71.48%. However, both parameters declined markedly with increasing storage time. The dissolved ozone concentration decreased to 0.28, 0.21, 0.13, and 0.10 mg/L after 15, 30, 45, and 60 min of storage, respectively, while the corresponding TCH removal efficiency dropped to approximately 12%, 4%, 1.5%, and nearly zero.

The progressive decrease in dissolved ozone reflects its inherently limited stability in aqueous media, where it continuously undergoes self-decomposition and reacts with dissolved nitrogen species and other plasma-generated oxidants. These reactions gradually consume the long-lived reactive species responsible for the oxidative capacity of plasma-activated water, resulting in a continuous loss of degradation performance during storage (Zhou et al. 2020). The close correlation between the decay of dissolved ozone and the reduction in TCH removal efficiency indicates that ozone plays a dominant role in preserving the oxidative activity of PAW. Therefore, although other long-lived oxidants may also contribute to pollutant degradation, the results clearly demonstrate that freshly prepared PAW should be used immediately after generation to maximize treatment efficiency and minimize the loss of reactive species during storage.

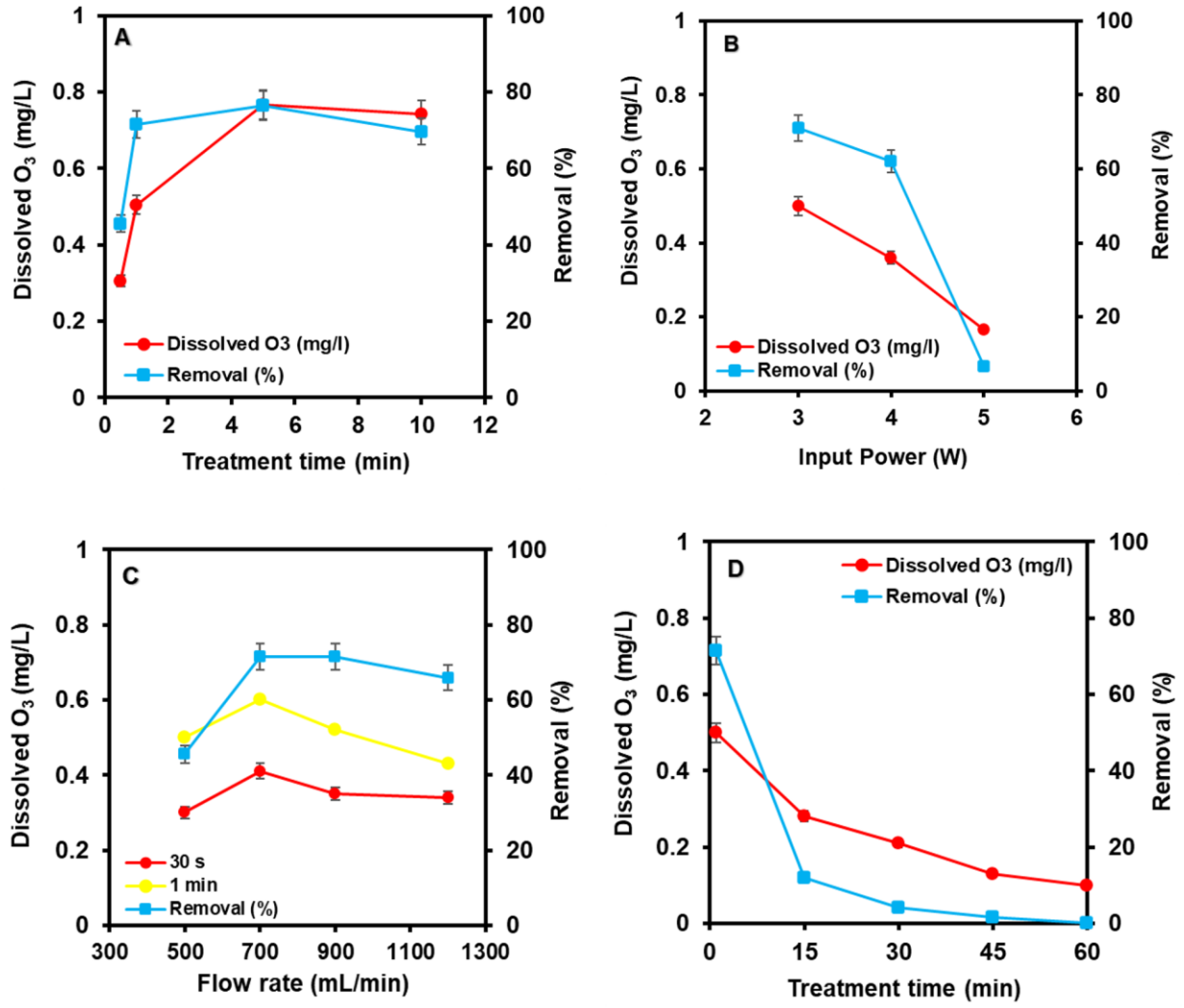


Fig. 7. *(A) Variation of dissolved ozone concentration in plasma-activated water as a function of plasma activation time at an input power of 3 W and an air flow rate of 500 mL/min. (B) Effect of input power on dissolved ozone concentration at a treatment time of 1 min and an air flow rate of 500 mL/min. (C) Effect of air flow rate on dissolved ozone concentration after plasma activation times of 30 s and 1 min, together with the corresponding TCH removal efficiency obtained after 30 s of plasma activation in 3 W. (D) Storage stability of dissolved ozone and the corresponding TCH removal efficiency in plasma-activated water generated under the optimum operating conditions (3 W, 700 mL/min, and 30 s).*

3.5 Effect of Reactive Nitrogen Species

Besides oxygen-derived oxidizing agents, nitrogen-based reactive species generated during air plasma discharge also influence the chemical composition and reactivity of plasma-activated water

(PAW). In atmospheric air plasma systems, nitrogen molecules interact with atomic oxygen and excited oxygen species within the discharge region, leading to the formation of nitrogen oxides (NO_x). These nitrogen oxides originate primarily from the initial formation of nitric oxide (NO), which is produced through reactions between nitrogen and oxygen species under energetic plasma conditions. Subsequently, NO is rapidly oxidized to nitrogen dioxide (NO_2) through reactions with molecular oxygen or ozone, as described in Eqs. (5) and (6) (Li et al. 2015):

$$2NO + O_2 \rightarrow 2NO_2 \qquad (5)$$

$$NO + O_3 \rightarrow NO_2 + O_2 \qquad (6)$$

Gas-phase measurements indicated that the concentration of NO remained negligible under the investigated plasma conditions, suggesting that NO undergoes rapid conversion to NO_2 immediately after formation. Once transferred into the liquid phase, NO_2 and any residual NO interact with water molecules, producing nitrite (NO_2^-) and nitrate (NO_3^-) ions according to Eqs. (7) and (8) (Pârvulescu et al. 2012):

$$2NO_2(aq) + H_2O \rightarrow NO_2^- + NO_3^- + 2H^+ \qquad (7)$$

$$NO_2(aq) + NO(aq) + H_2O \rightarrow 2NO_2^- + 2H^+ \qquad (8)$$

The nitrite ions accumulated in PAW originate mainly from the dissolution of nitrogen oxides formed through N_2–O_2 interactions in the plasma discharge region. In the presence of strong oxidants such as ozone and hydrogen peroxide, nitrite may undergo further oxidation to nitrate, thereby altering the balance of reactive species in the aqueous phase (Zhou et al. 2015).

Fig. 8A illustrates the variation of gas-phase NO_2 concentration as a function of input power at a constant air flow rate of 500 mL/min. As the input power increased from 3 to 5 W, the NO_2

concentration decreased markedly, dropping from approximately 115 mg/L at 3 W to about 72 mg/L at 4 W and further declining to nearly 25 mg/L at 5 W. This reduction can be attributed to the rapid increase in local gas temperature associated with higher power levels, which destabilizes nitrogen oxide species and accelerates their decomposition into less reactive forms with lower oxidation potential (Wang et al. 2020). The observed decrease in NO_2 concentration at elevated power levels is consistent with the simultaneous decline in TCH removal efficiency under these conditions.

The influence of air flow rate on NO_2 formation at an input power of 3 W is presented in Fig. 8B. Increasing the air flow rate from 500 to 900 mL/min resulted in a significant rise in NO_2 concentration, from approximately 115 mg/L to nearly 175 mg/L. This enhancement can be attributed to the increased availability of nitrogen and oxygen molecules within the discharge region, which promotes NO_x generation through electron-impact reactions and radical interactions (Cimerman and Hensel 2023; Segura et al. 2025). However, when the flow rate was further increased to 1200 mL/min, the NO_2 concentration decreased to around 155 mg/L. At excessively high flow rates, the residence time of gas molecules in the plasma zone becomes shorter, limiting their exposure to energetic electrons and excited species and thereby reducing the efficiency of NO_x formation (Chonpan et al. 2025; Marcinauskas et al. 2025).

Although reactive nitrogen species contribute to the acidification of PAW and influence the overall chemical environment, their direct oxidation capability toward organic pollutants is generally weaker than that of oxygen-based oxidants such as ozone and hydroxyl radicals. Nevertheless, the highest NO_2 concentration was observed at an air flow rate of 900 mL/min, which coincides with the condition that produced the maximum TCH removal efficiency. This observation suggests that the degradation performance is governed by the combined effects of reactive nitrogen species,

dissolved ozone, and improved gas–liquid interaction. The simultaneous optimization of these factors at 900 mL/min, therefore, explains why this flow rate represents the most favorable operational condition for TCH degradation in the present plasma system.

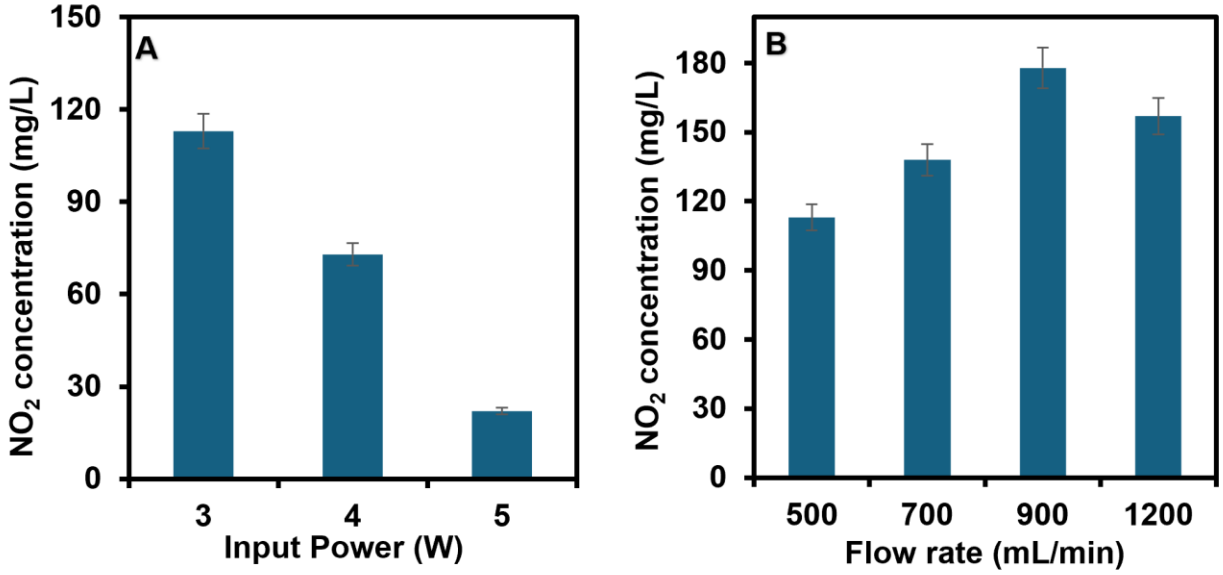


Fig. 8. (A) Variation of NO_2 concentration in the gas phase as a function of input power at a constant air flow rate of 500 mL/min. (B) Effect of air flow rate on NO_2 concentration in the gas phase at an input power of 3 W.

Conclusion

In this study, the performance of plasma-activated water produced by a multi-array atmospheric dielectric barrier discharge plasma jet diffuser was investigated for the degradation of tetracycline hydrochloride in aqueous solution. The operational parameters of the reactor were systematically optimized in order to achieve the highest pollutant degradation efficiency together with improved energy performance while also examining the formation of reactive species responsible for the

oxidation process. The results demonstrated that reactor operating conditions strongly influence both the generation of reactive oxygen and nitrogen species and the overall treatment efficiency. Increasing the input power and gas flow rate altered the plasma–liquid interaction and affected the production and stability of oxidative species such as ozone and other reactive radicals that play a critical role in the degradation of tetracycline molecules. The experimental analysis revealed that appropriate control of the operating parameters significantly improves treatment performance. Under the optimal operational conditions consisting of an input power of 3 W, an air flow rate of 700 mL/min, a processing time of 30 s, and a solution volume of 100 mL, the system achieved a tetracycline removal efficiency of 71.48 percent with an energy efficiency of approximately 20 g/kW.h . These results indicate that effective pollutant degradation can be obtained under relatively low power consumption when the plasma discharge conditions and gas–liquid interaction are properly adjusted. The investigation of reactive species further confirmed that the oxidative capacity of the generated plasma-activated water is primarily associated with the formation of strong oxidants produced during the plasma activation process, which participate in the breakdown of tetracycline molecules through advanced oxidation pathways. Overall, the findings demonstrate that the proposed plasma jet diffuser reactor provides an efficient and energy-effective approach for the treatment of pharmaceutical contaminants in water. The optimized operating conditions enable substantial degradation of tetracycline while maintaining favorable energy efficiency, highlighting the potential of plasma-based advanced oxidation processes as promising technologies for sustainable water and wastewater treatment applications.

Funding Declaration

The authors received no specific funding for this work from any funding agency in the public, commercial, or not-for-profit sectors.

Declaration of generative AI and AI-assisted technologies in the manuscript preparation process

During the preparation of this work, the authors used ChatGPT (OpenAI) to improve the language, grammar, and readability of the manuscript. In addition, ChatGPT (OpenAI) was used to assist in the preparation of the graphical abstract and the schematic illustration of the experimental reactor to improve the clarity and visual presentation of the study. After using this service, the authors reviewed and edited all generated content as needed and took full responsibility for the content of the published article.

Data Availability

The datasets generated and/or analyzed during the current study are available from the corresponding author upon reasonable request.

References:

Aboubakr HA, Gangal U, Youssef MM, et al (2016) Inactivation of virus in solution by cold atmospheric pressure plasma: identification of chemical inactivation pathways. J Phys D Appl Phys 49:204001

Al-Sharify ZT, Al-Sharify TA, al-Azawi AM, others (2020) Investigative study on the interaction and applications of plasma activated water (PAW). In: IOP Conference Series: Materials Science and Engineering. p 12042

Alegria F (2023) Using digital methods in active power measurement. Acta IMEKO. https://doi.org/10.21014/actaimeko.v12i4.1590

Ali S, Khalil AAK, Akhtar MS, et al (2026) Comprehensive insights into natural bioactive compounds: from chemical diversity and mechanisms to biotechnological innovations and applications. ChemistryOpen 15:e202500469

Amparán MAA, Palacios A, Flores GM, Olivera PMC (2025) Review and future outlook for the removal of microplastics by physical, biological and chemical methods in water bodies and wastewaters. Environ Monit Assess 197:429

Bader H (1982) Determination of Ozone In Water By The Indigo Method: A Submitted Standard Method. Ozone-science Eng 4:169–176. https://doi.org/10.1080/01919518208550955

Basu-Modak S, Ali D, Gordon M, et al (2006) Suppression of UVA-mediated release of labile iron by epicatechin-A link to lysosomal protection. Free Radic Biol Med 41:1197–1204. https://doi.org/10.1016/j.freeradbiomed.2006.06.008

Ben Amor I, Hemmami H, Zeghoud S, et al (2025) Cold plasma technology in wastewater

treatment: mechanisms, applications, and key challenges for organic pollutant removal. Int J Environ Sci Technol 22:10895–10912

Chen G, Zhou M, Chen S, Chen W (2009) The different effects of oxygen and air DBD plasma byproducts on the degradation of methyl violet 5BN. J Hazard Mater 172:786–791

Chen H, Zhai J, Ji Y, et al (2026) Review on Process Intensification of Non-Thermal Plasma Oxidation in Multiphase Reactor for Wastewater Treatment: Mass Transfer Enhancement and Waste Energy-Driven Conversion. Water 18:649

Chen J, Du Y, Shen Z, et al (2017) Non-thermal plasma and BiPO4 induced degradation of aqueous crystal violet. Sep Purif Technol 179:135–144

Chonpan P, Theinnoi K, Iamcheerangkoon T, et al (2025) Effects of operating parameters on dielectric barrier discharge non-thermal plasma ozone generator performance and NO Conversion. E3S Web Conf. https://doi.org/10.1051/e3sconf/202561004001

Cimerman R, Hensel K (2023) Multi-hollow Surface Dielectric Barrier Discharge: Production of Gaseous Species Under Various Air Flow Rates and Relative Humidities. Plasma Chem Plasma Process 43:1411–1433. https://doi.org/10.1007/s11090-023-10381-4

Crini G, Mongiov\'\i C, Lichtfouse É, et al (2026) Advantages and disadvantages of separation-based water treatment methods for the removal of per-and polyfluoroalkyl substances in drinking water: a review. Environ Chem Lett 24:321–345

Dolatimehr A, Mahyar A, Barough SPH, Mahmoodi M (2024) Insights into the efficiencies of different biological treatment systems for pharmaceuticals removal: A review. Water Environ Res 96:e11153

Elaissi S, Alsaif NAM (2023) Modelling of nonthermal dielectric barrier discharge plasma at atmospheric pressure and role of produced reactive species in surface polymer microbial purification. Polymers (Basel) 15:1235

Ethiraj S, Samuel MS, others (2024) A comprehensive review of the challenges and opportunities in microalgae-based wastewater treatment for eliminating organic, inorganic, and emerging pollutants. Biocatal Agric Biotechnol 60:103316

Griffero L, Frontera P, Silva B, et al (2026) Assessment of Emerging Contaminants in Wastewater Treatment Plants and Receiving Surface Waters from Uruguay. ACS ES\&T Water

Hao C, Yan Z, Liu K, Qiu J (2020) Degradation of pharmaceutical contaminant tetracycline in aqueous solution by coaxial-type DBD plasma reactor. IEEE Trans Plasma Sci 48:471–481

He D, Sun Y, Xin L, Feng J (2014) Aqueous tetracycline degradation by non-thermal plasma combined with nano-TiO2. Chem Eng J 258:18–25

Hidayatullah IM, Steven S, Kusmayadi A, et al (2025) Advances in antibiotic biodegradation: emerging strategies and challenges in mitigating environmental contamination and resistance. Curr Pollut Reports 11:35

Hossaini H, Pirsaheb M, Hossini H, et al (2024) Improving the purification of aqueous solutions by controlling the production of reactive oxygen species in non-thermal plasma; a systematic review. Rev Environ Health 39:199–209

Hosseini MM, Taghvaei H (2025) Efficient treatment of graywater using a multi-array dielectric barrier discharge plasma jet. J Water Process Eng 76:108178

Huang J, Puyang C, Wang Y, et al (2022) Hydroxylamine activated by discharge plasma for

synergetic degradation of tetracycline in water: Insight into performance and mechanism. Sep Purif Technol 300:121913

Islam IU, Qurashi AN, Adnan A, et al (2025) Bioremediation and adsorption: strategies for managing pharmaceutical pollution in aquatic environment. Water, Air, \& Soil Pollut 236:579

Jiang B, Zheng J, Liu Q, Wu M (2012) Degradation of azo dye using non-thermal plasma advanced oxidation process in a circulatory airtight reactor system. Chem Eng J 204:32–39

Jo J-O, Moon SH, Mok YS (2015) Non-thermal plasma degradation of dye using an underwater dielectric barrier discharge created inside a porous hydrophobic ceramic tube. Color Technol 131:73–80

Kayani KF (2025) Tetracycline in the environment: Toxicity, uses, occurrence, detection, and removal by covalent organic frameworks- Recent advances and challenges. Sep Purif Technol 364:132418

Kazemi M, Taghvaei H (2021) A novel multi array dielectric barrier discharge plasma gas diffuser for wastewater treatment: The role of reactive species. Sep Purif Technol 260:118236

Kumar P, Saxena P (2026) Plasma-Activated Water (PAW) for the Degradation of Organic Pollutants in Diluted Industrial Effluents. arXiv Prepr arXiv260101270

Kumar TN, Mohapatro S, Dash RR (2024) Removal of dyes from aqueous solutions using non-thermal plasma: a review. Int J Environ Sci Technol 21:7819–7836

Levanov A V, Isaikina OY, Lunin V V (2019) Thermodynamic and kinetic parameters of the solubility of ozone in water. Russ J Phys Chem A 93:1230–1234

Li B, Zhao J, Lu J (2015) Numerical Study of the Simultaneous Oxidation of NO and SO2 by Ozone. Int J Environ Res Public Health 12:1595–1611. https://doi.org/10.3390/ijerph120201595

Li Q, Zheng Y, Guo L, et al (2024) Microbial degradation of tetracycline antibiotics: mechanisms and environmental implications. J Agric Food Chem 72:13523–13536

Lou J, Wei Y, Zhang M, et al (2021) Removal of tetracycline hydrochloride in aqueous by coupling dielectric barrier discharge plasma with biochar. Sep Purif Technol 266:118515

Łukasiewicz E (2025) Coagulation--Sedimentation in Water and Wastewater Treatment: Removal of Pesticides, Pharmaceuticals, PFAS, Microplastics, and Natural Organic Matter. Water 17:3048

Lunder M, Dahle S, Fink R (2025) Cold Atmospheric Plasma for Water Disinfection: Mechanisms, Efficacy and Resistant Bacteria Inactivation. Plasma Process Polym 22:70050

Mandlazi NB, Vilakati GD, Madikizela L, Kgomo H (2026) Non-targeted screening of emerging pollutants across wastewater and receiving waters: A case study in Eswatini. Sci Total Environ 1014:181353

Marcinauskas L, Uscila R, Aikas M (2025) The Influence of Air Flow Rates and Voltage on the Plasma Emission Spectra and the Concentrations of Nitrogen Oxides Produced by Gliding Arc Discharge Plasma. Appl Sci. https://doi.org/10.3390/app15010446

Mbanugo VS, Ojo BS, Lin TC, et al (2025) Per-and polyfluoroalkyl substance (PFAS) degradation in water and soil using cold atmospheric plasma (CAP): a review. ACS Phys Chem Au 5:117–133

Minesi N, Blanchard V, Pannier E, et al (2022) Plasma-assisted combustion with nanosecond discharges. I: Discharge effects characterization in the burnt gases of a lean flame. Plasma Sources Sci Technol 31:. https://doi.org/10.1088/1361-6595/ac5cd4

Mok YS, Jo J-O, Whitehead JC (2008) Degradation of an azo dye Orange II using a gas phase dielectric barrier discharge reactor submerged in water. Chem Eng J 142:56–64

Naudé N, Cambronne JP, Gherardi N, Massines F (2005) Electrical model and analysis of the transition from an atmospheric pressure Townsend discharge to a filamentary discharge. J Phys D Appl Phys 38:530–538

Ouzar A, Goutomo BT, Nam K, Kim I-K (2025) Efficient removal of tetracycline antibiotic by nonthermal plasma-catalysis combination process. Environ Eng Res 30:

Ouzar A, Kim I-K (2022) Tetracycline degradation by nonthermal plasma: removal efficiency, degradation pathway, and toxicity evaluation. Water Sci \& Technol 86:2794–2807

Pârvulescu VI, Magureanu M, Lukes P (2012) Plasma chemistry and catalysis in gases and liquids. John Wiley \& Sons

Rahimpour M, Taghvaei H, Rahimpour MR (2019) Degradation of crystal violet in water solution using post discharge DBD plasma treatment: Factorial design experiment and modeling. Chemosphere 232:213–223

Rasool BS, Abbas AK, Haddad R (2025) Photocatalytic innovations in environmental remediation: mechanisms, materials, and challenges for persistent organic pollutant removal. Environ Monit Assess 197:1086

Rezaee E, Hatam G, Zomorodian K, et al (2026) Leishmanicidal Efficacy of Cold Atmospheric

Multiple Plasma Jet against Leishmania major in a Murine Model: Effects on Parasite Burden, Cytokine Profiles, and Wound Healing

Satyam S, Patra S (2025) The evolving landscape of advanced oxidation processes in wastewater treatment: challenges and recent innovations. Processes 13:987

Segura ANT, Ikuse K, Hamaguchi S, et al (2025) Influence of gas flow rate on modes of reactive oxygen and nitrogen species in a grid-type surface dielectric barrier discharge. J Appl Phys. https://doi.org/10.1063/5.0265368

Semenova Y, Makalkina L, Glushkova N, Gaipov A (2025) Tetracyclines in the modern era: global consumption, antimicrobial resistance, environmental occurrence, and degradation techniques. Antibiotics 14:1183

Silva JA (2025) Advanced Oxidation Process in the Sustainable Treatment of Refractory Wastewater: A Systematic Literature Review. Sustain 17:

Solouki M, Ghobadi-Nejad Z, Ghasemian S, Yaghmaei S (2026) Enhancement of biological treatment of levofloxacin through electrochemical oxidation as a pretreatment. Int J Environ Sci Technol 23:28

Thirumdas R, Kothakota A, Annapure U, et al (2018) Plasma activated water (PAW): Chemistry, physico-chemical properties, applications in food and agriculture. Trends food Sci \& Technol 77:21–31

Wang L, Yu L, Cai B (2024) Characteristics of tetracycline antibiotic resistance gene enrichment and migration in soil--plant system. Environ Geochem Health 46:427

Wang X, Huang Q, Ding S, et al (2020) Micro hollow cathode excited dielectric barrier discharge

(DBD) plasma bubble and the application in organic wastewater treatment. Sep Purif Technol 240:116659

Wang Y, Liu Y, Zhang H, et al (2025) Carbonaceous materials in structural dimensions for advanced oxidation processes. Chem Soc Rev 54:2436–2482

Wu M-C, Liu C-T, Chiang C-Y, et al (2018) Inactivation effect of Colletotrichum gloeosporioides by long-lived chemical species using atmospheric-pressure corona plasma-activated water. IEEE Trans Plasma Sci 47:1100–1104

Xu Y, Bassi A (2025) Non-thermal plasma decontamination of microbes: a state of the art. Biotechnol Prog 41:e3511

Yang CAO, Tengfei LI, Tiecheng W, others (2018) Review on reactive species in water treatment using electrical discharge plasma: formation, measurement, mechanisms and mass transfer. Plasma Sci Technol 20:103001

Zhou R, Zhang X, Bi Z, et al (2015) Inactivation of Escherichia coli cells in aqueous solution by atmospheric-pressure N2, He, Air, and O2 microplasmas. Appl Environ Microbiol 81:5257–5265

Zhou R, Zhou R, Wang P, et al (2020) Plasma-activated water: Generation, origin of reactive species and biological applications. J Phys D Appl Phys 53:303001

Zou F, Yang M, Wu J, et al (2025) The potential of plasma-activated water in safe and sustainable food production: a comprehensive review of recent advances and future trends. Crit Rev Food Sci Nutr 1–25